Numerical solution of convection-dominated diffusion problem using modified upwind finite volume method

Arafat Hussain[1], Zhoushun Zheng*[1], Eyaya Fekadie Anley[1,2]

[1] *School of Mathematics and Statistics, Central South University, Changsha, 410083, China.*

[2] *Department of Mathematics, College of Natural and Computational Science, Arba-Minch 21, Ethiopia.*

Abstract

In this paper, an attempt has been made to developed a numerical scheme for numerical approximation of the convection-diffusion problem in convection dominant situations. Applying Lagrange interpolation technique, new expressions are obtained to approximate the variable at spatial interfaces of the computational domain. Subsequently, these interface approximations are used to developed a numerical scheme based on upwind approach in the finite volume method. Crank-Nicolson technique is used for the approximation along temporal direction. This newly constructed numerical scheme is unconditionally stable with second order accuracy along space and time both. The numerical experiments are performed using the proposed upwind approach and numerical results confirm the theoretical algorithm. Numerical results produce by our constructed numerical are compared with conventional finite volume method. This comparison indicates for convection dominant phenomena the numerical solution of conventional finite volume method contains with non-physical oscillations where are our proposed numerical schemes give a high accurate and stable solution.

Keywords: Lagrange interpolation, convection diffusion, spatial interface, upwind finite volume method.

2020 MSC: 35Cxx, 35Dxx, 35Nxx.

1. Introduction

The convection-diffusion equation is a basic governing problem to represent the transport phenomena of any property. These transport phenomena have arised in many fields like industry, biology, agriculture, petrochemistry and meteorology. Mathematical modelling of transport phenomena, pollutants, and suspended matter in water and soil involves the numerical solution of a convection-diffusion problem as we have seen in [1, 2, 3, 4, 5, 6, 7]. Mathematical models representing any transport phenomena, are given by systems of second-order partial differential equations that contain terms describing convection and diffusion of a fluid in medium. The convection is define by first-order terms while the diffusion of property is described by second-order term. The convection-diffusion equation can be driven in a straightforward way from the equation of continuity, which states that the rate of change for a scalar quantity in a differential control volume is given by convection and diffusion in and out along with any source or sink inside the control volume[8, 9]. These governing equations can not be solved using any analytical approach. Due to this reason, it is essential to apply different numerical methods to find out numerical solution for such problems. Finite difference method (FDM), finite element methods (FEM) and finite volume methods (FVM) are three most popular and widely used numerical techniques for approximation of such governing problems.

The finite difference method (FDM) studied by [10, 11, 12, 13, 14, 15, 16] is a domain discretising technique, convert the governing problem into a difference equation. The functional values are approximated at the nodes of the network. Finite difference method is applied to the basic conservation equations in laminar film boiling and conclude that, the rate of convergence of finite-difference equations is dependent on the conditions in the liquid region. By using the over-relaxation technique in the liquid region, the rate of convergence was accelerated by [17]. An efficient parallel characteristic scheme of finite difference method is proposed for numerical simulation of convection-diffusion equation[18]. The advantage of numerical approach of this study is that, only one are two iterations are needed to obtain the optimal accuracy at each time level. In [19], finite difference method is applied to a system of simultaneous

*Corresponding author

Email addresses: arafathussain@csu.edu.cn (Arafat Hussain[1]), 2009zhengzhoushun@163.com (Zhoushun Zheng*[1]), eyayafek@csu.edu.cn/efekadie9@gmail.com (Eyaya Fekadie Anley[1,2])

non-linear partial differential equations which represents the transport phenomena when a fluid evaporates from the hot wall and condenses on the cold wall of an upright rectangular cavity. This study concludes that, a constraint is needed on the physical parameters of the problem in order to achieve the existence of a solution of the steady state problem. A high order finite difference strategy based on Richardson extrapolation and operator interpolation is proposed for solving convection-diffusion equation in [20]. For a limiting case where mesh-size and viscosity approach to zero, a numerical scheme based on finite difference method is discussed for numerical simulation of singularly perturbed convection problem [21]. A numerical simulation to study the convection and diffusion mechanism on the cylinder husk furnace using finite difference method is discussed. Based on this study, the transport phenomena in the cylinder husk furnace is convection dominated as treated by [22]. A compact finite difference method is applied to solve unsteady convection-diffusion equation in [23]. In this new approach, first the convection-diffusion equation is transformed to the reaction-diffusion equation, and then it is solved by proposed unconditionally stable numerical method. As we have studied in [24], a nine-point compact discretization strategy has been used in conjunction with the multi-grid algorithm to obtain a highly accurate numerical solution of the convection-diffusion equation. A minimal residual smoothing(MRS) technique is discussed to accelerate this multi-grid formulation. Finite difference techniques using spreadsheets are applied to approximate the one dimensional advection-diffusion equation (see [25] the details). Numerical approximation of different finite difference schemes are compared with analytical solution of the problem.

Finite Element Method which discussed in [26, 27, 28, 29, 30] is another numerical method used for numerical approximation of the governing problems. The potential of this method has revived interest in the past few years in the solution of differential equations. For convection diffusion problem, using finite element method a local error estimates are derived and shown that, the analysis can be applied in parallel fashion to the discontinuous Galerkin method[31]. In the study [32] with piecewise polynomials of degree $n \geq 2$ an explicit form of finite element method is presented for time dependent convection diffusion problem. The proposed method employs space-time elements and allowing the numerical solution to be computed one element at a time. A technique based on finite element method is introduced for hyperbolic problems, which also extended to steady state convection dominated convection-diffusion problem[29]. The constructed method can be applied in explicit fashion, which is sufficiently stable for small mesh-size (h) and complement to Galerkin method in the convection dominant regime. In [33] for one dimensional convection-diffusion problem, convergence properties of finite element method with moving nodes along characteristics are discussed. Linear and non-linear both problems are focused. For linear elements, optimal rates of convergence order with different norms are studied. Finite element method is applied to discretized unsteady convection diffusion equation by [34]. Resultant matrix system is solved by using conjugate gradient method, which improve computational time and memory size. A form of weak finite element method is applied to approximate convection diffusion equation is implemented in [35]. The optimal order error estimates are derived in different discrete norms. Finite element approximation [36] for a singularly perturbed one dimensional convection-diffusion equation are constructed. The Local error indicators and Local bounds provides a basis for self adaptive mesh refinement. For convection-diffusion boundary value problem, Galerkin piecewise linear finite element method is considered which is second order accurate. To generate a discrete linear algebraic system special formulae is applied, which take the boundary layer character of the solution into account [37]. With several novel features including a streamline upwind formulation for the advection terms and equal order interpolations for all variables a new finite element method is presented [38]. The formulation proposed in this study shows, flexibility in terms of geometry and boundary conditions, and the results obtained from this finite element formulation illustrate its ability to accurately predict the fluid properties in both forced and free convection flows. In [39] a finite element formulation for numerical modelling of porous medium flow is presented. In this study both the semi- and quasi- implicit schemes are used to solve many problems. Mostly the results presented are highly accurate and consistent with the experimental and other numerical data.

Since in flow simulation, it is very important to satisfy conservation laws at all levels, by avoiding generation and consumption of property due to artificial terms inside control volume which is not guaranteed in finite difference method(FDM) and finite element method(FEM). Finite volume method (FVM) [40, 41, 42, 43, 44] is evolved from the finite differences method, which is flexible and widely employed in fluid dynamics. Finite volume method is integration based technique in which using the divergence theorem, volume integrals in governing problem that contain

divergence terms are converted to surface integrals. This control volume integration is key step in finite volume method(FVM), which ensured the conservation of relevant variable at each finite control cell level. This control volume integration gives a semi–discretize conservation law which involves fluxes at the interfaces of control volumes which are need to approximate and this interface approximation converts partial differential equation into a set of algebraic equations. In the past Based on different choices to these interface approximations several numerical techniques of finite volume method (FVM) formulation are developed[45, 46, 47, 48, 49, 50]. The convection–diffusion equation can be either convection dominated or diffusion dominated, it depends on the rate of convection and the rate of diffusion. Many phenomena in engineering and science are governed by convection-dominated diffusion equations. In many applications recognized as convection dominated problems, diffusion may be quite small as compare to convection. In such cases standard numerical methods gives solution with spurious oscillations. To overcome this stability problem, various numerical methods have been proposed[51, 52, 53].. An exponentially fitted finite volume method is applied to approximate the convection-dominated anisotropic diffusion problem [54]. Authors in this study used a simple coordinate transformation to transform the problem with constant anisotropic diffusion matrix coefficient into problem with isotropic diffusion coefficient. The resulting problem is approximated by using exponentially fitted finite volume method. Adaptive mesh method is also a useful technique for solving convection dominate problems. Adaptive mesh refinement method and moving mesh refinement method are most popular adaptive mesh approaches. A self adaptive mesh is proposed to address the convection dominancy[55].

In our previous research paper [45], Taylor series formulation is applied for the approximation of variable at interface of computational domain and new upwind numerical formulation is proposed for numerical simulation of convection-diffusion problem. Whereas in current study, new expressions are obtained using Lagrange interpolation for approximation of variable at spatial interfaces of control volume. subsequently, using these interface approximations, a numerical scheme based of upwind approach formulation is constructed . This numerical scheme is unconditionally stable with second order accuracy in space and time. One of the most common and widely used techniques, the Crank–Nicolson method is applied for temporal approximation.

The format of this paper is organized as: A brief about mathematical model of convection-diffusion and domain discretization using finite volume method Section 2. In Section 3 mathematical formulation of modified upwind approach finite volume method is discussed. Section 4 deals about the analysis of stability and convergence order of our developed numerical approach, using the von Neumann–Fourier method. In Section 5 some numerical experiments are carried out to validate our theoretical algorithm and conclusion of this study is presented in Section 6.

2. Finite volume method and Mathematical model

The basic principle of all finite volume methods is to study the differential equation in conservative form, integrate it over small regions (called ”cells” or ”control volumes”), and convert each such integral into an integral over the boundary of the cell by means of Gauss’s theorem. In order to have the nodes of the grid at the centres of cells, we introduce a new rectangular grid whose nodes are the cell centres of the original grid which is shown in Figure 1. Nodal points are used within these control volumes for interpolating the field variable and usually, single node at the center of the control volume is used for each control volume. The finite volume method is a discretization of the governing equation in integral form, in contrast to the finite difference method, which is unusually applied to the governing equation in differential form. In order to obtain a finite volume discretization, the domain Ω will be

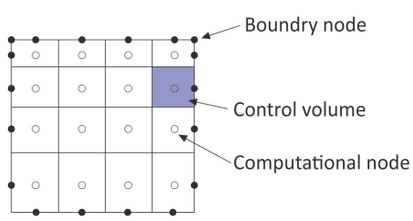

Figure 1: The indication for the place of nodes

sub–divided to M sub–domains Ω_i, $i = 1, 2, \cdots, M$ such that the collection of all those sub–domains forms a partition

of Ω, *i.e* as in [56],

(i). Each of the domain Ω_i is an open, connected and bounded set without slits.

(ii). There is no any common point between each sub–domains ($i.e \Omega_i \cap \Omega_j = \emptyset$ for $i \neq j$).

(iii). The union of all the sub-domain gives the domain of the region.($i.e \cup_{i=1}^{M} \Omega_i = \Omega$. These sub-domains Ω_i are called control volumes(CVs) or control domains (see Figure 2). In the finite volume formulation the first step is to divide the whole computational domain into finite number of sub–domain also called control volumes Ω_i. When we are talking about one-dimensional problems, we are considered the CVs as sub-intervals of the problem and the nodes can be the mid-points or the edges of the sub-intervals (see Figure 3). In the paper [], authors are assumed that $\Omega \subset R^d, d \geq 1$ be

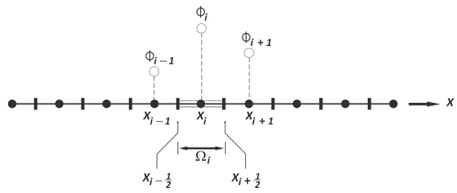

Figure 2: Discretization of the domain.

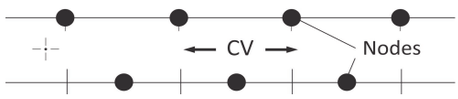

Figure 3: Definitions of CVs and edge (top) and cell-oriented (bottom) arrangement of nodes for One-dimensional grids

a bounded polygonal domain and let $T > 0$ be given, then the following initial- boundary value problem is given:

$$\begin{cases} \partial_t \phi + div(v\phi) + c\phi = 0, \ \ (x,t) \in \Omega \times [0,T], \\ \phi(x,0) = \phi_0(x), \ \ x \in \Omega, \\ \phi(0,t) = \phi_1(t), \ \ \phi(L,t) = \phi_2(t), \end{cases} \tag{1}$$

The analysis and discretization of these problem is treated by using upwind finite volume method. The work is discussed in the analysis of finite volume method for coupled systems in which transport like equation play a great role. when we make $c = 0$ and by adding the diffusion term, we have found our problem which is convection-dominated diffusion equation given by:

$$\begin{cases} \dfrac{\partial u(x,t)}{\partial t} + v\dfrac{\partial u(x,t)}{\partial x} = k\dfrac{\partial^2 u(x,t)}{\partial x^2} + Q(x,t), (x,t) \in \Omega \times (0,T], \\ \phi(x,0) = f(x), \ \ 0 \leq x \leq L, \\ \phi(0,t) = \phi_1(t), u(L,t) = \phi_2(t), \ \ 0 \leq t \leq T, \end{cases} \tag{2}$$

where $\Omega = (0,L), \ \ k \geq 0, \ \ v \geq 0$ are constant coefficients of diffusion and convection respectively, where as $\phi(x,t)$ is the field variable transported along x-direction which is unknown, $Q(x,t)$ represents sour term. The governing Eq.(1) is the model for the physical phenomena which have diffusion and transport. $v\frac{\partial \phi}{\partial x}$ represents the convective term or transport of the property where as $k\frac{\partial^2 \Phi}{\partial x^2}$ shows the diffusion term. The Peclet number ($Pe = \frac{v\Delta x}{k}$) describes the ratio of convection and diffusion equation which has more effect on the process. If this ratio is high then conventional numerical methods gives solution with non-physical oscillations.

3. Formulation and discretization

In these paper, we are restricted to uniform discretization and adjust the grid node x_i in the center of control volume. The interface Γ or common boundary of i^{th} control volume with its adjacent control volumes Ω_{i-1} and Ω_{i+1} are mostly positioned at the mid position between their centers i.e, $\Gamma_{i-\frac{1}{2}} = \frac{x_i + x_{i-1}}{2}$ and $\Gamma_{i+\frac{1}{2}} = \frac{x_i + x_{i+1}}{2}$. The space discretization with the uniform cell centred approach of finite volume method is considered. The spatial domain $[0,L]$ is divided into M equal control volumes of uniform length h. A mesh of M points between $[0,L]$ is considered, so that, $x_i = ih$ and Ω be the rectangle $[0,L] \times [0,T]$. D is meshed considering the points $\phi_{i,j}$ in the co-ordinate system (x_i, t_j). The width of spatial and temporal domain partition are respectively define as, $\Delta x = h = x_{i+1} - x_i$ and $\Delta t = t_{j+1} - t_j$. By integrating

the govern Equation (1) over the control volume $[x_{i-\frac{\Delta x}{2}}, x_{i+\frac{\Delta x}{2}}] \times [t_{j-1}, t_j]$ around node x_i.

$$\begin{aligned} & \int_{i-\frac{\Delta x}{2}}^{i+\frac{\Delta x}{2}} \int_{j-\frac{\Delta t}{2}}^{j+\frac{\Delta t}{2}} \frac{\partial \Phi}{\partial t} dt dx + v \int_{j-\frac{\Delta t}{2}}^{j+\frac{\Delta t}{2}} \int_{i-\frac{\Delta x}{2}}^{i+\frac{\Delta x}{2}} \frac{\partial \Phi}{\partial x} dx dt \\ = \quad & k \int_{j-\frac{\Delta t}{2}}^{j+\frac{\Delta t}{2}} \int_{i-\frac{\Delta x}{2}}^{i+\frac{\Delta x}{2}} \frac{\partial^2 \Phi}{\partial^2 x} dx dt. \end{aligned} \tag{3}$$

The first term is approximated by using trapezoidal rule for numerical integration:

$$\begin{aligned} & \frac{\Delta x}{2} \left(\phi_{i+\frac{\Delta x}{2}, j+\frac{\Delta t}{2}} + \Phi i - \frac{\Delta x}{2}, j + \frac{\Delta t}{2} \right) - \frac{\Delta x}{2} \left(\phi_{i+\frac{\Delta x}{2}, j-\frac{\Delta t}{2}} + \Phi_{i-\frac{\Delta x}{2}, j-\frac{\Delta t}{2}} \right) \\ + \quad & v \int_{j-\frac{\Delta t}{2}}^{j+\frac{\Delta t}{2}} \left(\Phi_{i+\frac{\Delta x}{2}, j} - \Phi_{i-\frac{\Delta x}{2}, j} \right) dt = k \int_{j-\frac{\Delta t}{2}}^{j+\frac{\Delta t}{2}} \left((\frac{\partial \Phi}{\partial x})_{i+\frac{\Delta x}{2}, j} - (\frac{\partial \Phi}{\partial x})_{i-\frac{\Delta x}{2}, j} \right) dt. \end{aligned} \tag{4}$$

In problems where fluid flow plays an important role, we must consider the effects of convection term over the process. Diffusion always occurs alongside convection in nature. So, here we are examined numerical technique to predict the convection dominancy or flow direction. A modified upwind approach is applied for the interface approximation of convective terms. As the flow is positive and it comes from the left of control volume, the positive directional flow the highly influential nodes for i^{th} control volume are node $i-1$ and $i-2$. By this way taking the flow direction under consideration, we applied the Lagrange interpolation over the i^{th} control volume and its highly influential nodes to approximate the variable at interfaces. Applying the Lagrange interpolation over the points $(x_{i-2}, \phi_{i-2}), (x_{i-1}, \phi_{i-1})$ and (x_i, ϕ_i) ,we have developed the following expression:

$$\phi(x) = \frac{(x-x_{i-1})(x-x_i)}{(x_{i-2}-x_{i-1})(x_{i-2}-x_i)} \phi_{i-2} + \frac{(x-x_{i-2})(x-x_i)}{(x_{i-1}-x_{i-2})(x_{i-1}-x_i)} \phi_{i-1} + \frac{(x-x_{i-2})(x-x_{i-1})}{(x_i-x_{i-2})(x_i-x_{i-1})} \phi_i. \tag{5}$$

We have substituted $x = x_{i+\frac{\Delta x}{2}}$ in Equation (5) for approximation at east interface of control volume as:

$$\phi_{i+\frac{\Delta x}{2}} = \frac{3}{8}\phi_{i-2} - \frac{5}{4}\phi_{i-1} + \frac{15}{8}\phi_i. \tag{6}$$

This Equation (6) show our approximation for convective terms at east interface, using the highly influential nodes of a control volume for positive directional flow. Here the substitution of $x = x_{i-\frac{\Delta x}{2}}$ in Equation (5) for the approximation at west interface of control volume gives:

$$\phi_{i-\frac{\Delta x}{2}} = -\frac{1}{8}\phi_{i-2} + \frac{3}{4}\phi_{i-1} + \frac{3}{8}\phi_i. \tag{7}$$

This Equation (7) shows our approximation for convective terms at west interface, using the highly influential nodes of a control volume for positive directional flow. Central difference technique is used from the approximation of variable gradients at east and west interface of control volume,

$$\left(\frac{\partial \phi}{\partial x} \right)_{i+\frac{\Delta x}{2}} = \left(\frac{\phi_{i+1} - \phi_i}{\Delta x} \right) + O(\Delta x^2). \tag{8}$$

$$\left(\frac{\partial \phi}{\partial x} \right)_{i-\frac{\Delta x}{2}} = \left(\frac{\phi_i - \phi_{i-1}}{\Delta x} \right) + O(\Delta x^2). \tag{9}$$

Now by substituting Equation(6)- (9) in Equation (4), it becomes,

$$\begin{aligned} & \frac{\Delta x}{2} \left(\frac{1}{4}\phi_{i-2,j+1} - \frac{1}{2}\phi_{i-1,j+1} + \frac{9}{4}\phi_{i,j+1} \right) - \frac{\Delta x}{2} \left(\frac{1}{4}\phi_{i-2,j} - \frac{1}{2}\phi_{i-1,j} + \frac{9}{4}\phi_{i,j} \right) \\ + \quad & v \int_j^{j+1} \left(\frac{1}{2}\phi_{i-2} - 2\phi_{i-1} + \frac{3}{2}\phi_i \right) dt = k \int_j^{j+1} (\phi_{i-1} - 2\phi_i + \phi_{i+1})\, dt. \end{aligned} \tag{10}$$

Divide by Δx and after some arrangements Equation (10) can be written,

$$\begin{aligned} & \left(\frac{1}{8}\phi_{i-2,j+1} - \frac{1}{4}\phi_{i-1,j+1} + \frac{9}{8}\phi_{i,j+1} \right) + \left(\frac{v}{2\Delta x} \right) \int_j^{j+1} \phi_{i-2} dt + \left(\frac{-2v}{\Delta x} - \frac{k}{\Delta x^2} \right) \int_j^{j+1} \phi_{i-1} dt \\ + \quad & \left(\frac{3v}{2\Delta x} + \frac{2k}{\Delta x^2} \right) \int_j^{j+1} \phi_i dt + \left(-\frac{k}{\Delta x^2} \right) \int_j^{j+1} \phi_{i+1} dt = \left(\frac{1}{8}\phi_{i-2,j} - \frac{1}{4}\phi_{i-1,j} + \frac{9}{8}\phi_{i,j} \right) \end{aligned} \tag{11}$$

Here, we are applied θ scheme for the approximation along temporal direction as follows,

$$\int_j^{j+1} \phi_i dt = \left(\theta \phi_i^{j+1} + (1-\theta)\phi_i^j \right) \Delta t. \qquad \theta \in [0,1] \tag{12}$$

Applying this θ scheme over each node $i-2, i-1, i$ and node $i+1$ in Equation (11) and also after some simplification we get the following expression:

$$\begin{aligned}
& \left(\frac{1}{8}\phi_{i-2,j+1} - \frac{1}{4}\phi_{i-1,j+1} + \frac{9}{8}\phi_{i,j+1}\right) \\
+ \quad & \theta\left((\frac{v}{2\Delta x})\phi_{i-2,j+1} + (\frac{-2v}{\Delta x} - \frac{k}{\Delta x^2})\phi_{i-1,j+1} + (\frac{3v}{2\Delta x} + \frac{2k}{\Delta x^2})\phi_{i,j+1} + (-\frac{k}{\Delta x^2})\phi_{i+1,j+1}\right) \\
+ \quad & (1-\theta)\left((\frac{v}{2\Delta x})\phi_{i-2,j} + (\frac{-2v}{\Delta x} - \frac{k}{\Delta x^2})\phi_{i-1,j} + (\frac{3v}{2\Delta x} + \frac{2k}{\Delta x^2})\phi_{i,j} + (-\frac{k}{\Delta x^2})\phi_{i+1,j}\right) \\
= \quad & \left(\frac{1}{8}\phi_{i-2,j} - \frac{1}{4}\phi_{i-1,j} + \frac{9}{8}\phi_{i,j}\right)
\end{aligned} \tag{13}$$

For Crank-Nicolson scheme we have taken $\theta = \frac{1}{2}$ and get the result,

$$\begin{aligned}
& \left(\frac{1}{8} + \frac{v\Delta t}{4\Delta x}\right)\phi_{i-2}^{j+1} + \left(-\frac{1}{4} - \frac{v\Delta t}{\Delta x} - \frac{k\Delta t}{2\Delta x^2}\right)\phi_{i-1}^{j+1} + \left(\frac{9}{8} + \frac{3v\Delta t}{4\Delta x} + \frac{k\Delta t}{\Delta x^2}\right)\phi_i^{j+1} + \left(\frac{-k\Delta t}{2\Delta x^2}\right)\phi_{i+1}^{j+1} \\
= \quad & \left(\frac{1}{8} - \frac{v\Delta t}{4\Delta x}\right)\phi_{i-2}^{j} + \left(-\frac{1}{4} + \frac{v\Delta t}{\Delta x} + \frac{k\Delta t}{2\Delta x^2}\right)\phi_{i-1}^{j} + \left(\frac{9}{8} - \frac{3v\Delta t}{4\Delta x} - \frac{k\Delta t}{\Delta x^2}\right)\phi_i^{j} + \left(\frac{k\Delta t}{2\Delta x^2}\right)\phi_{i+1}^{j}
\end{aligned} \tag{14}$$

This Equation (14) show the fully descretized form of our new constructed numerical scheme for interior node from node $i-2$ to node $M-1$. In simplified form this expression can be put as:

$$C_1\phi_{i-2}^{j+1} + C_2\phi_{i-1}^{j+1} + C_3\phi_i^{j+1} + C_4\phi_{i+1}^{j+1} \quad = \quad C_5\phi_{i-2}^{j} + C_6\phi_{i-1}^{j} + C_7\phi_i^{j} + C_8\phi_{i+1}^{j}. \tag{15}$$

Where coefficients are given,

$C_1 = \left(\frac{1}{8} + \frac{v\Delta t}{4\Delta x}\right), C_2 = \left(-\frac{1}{4} - \frac{v\Delta t}{\Delta x} - \frac{k\Delta t}{2\Delta x^2}\right), C_3 = \left(\frac{9}{8} + \frac{3v\Delta t}{4\Delta x} + \frac{k\Delta t}{\Delta x^2}\right), C_4 = \left(\frac{-k\Delta t}{2\Delta x^2}\right),$
$C_5 = \left(\frac{1}{8} - \frac{v\Delta t}{4\Delta x}\right), C_6 = \left(-\frac{1}{4} + \frac{v\Delta t}{\Delta x} + \frac{k\Delta t}{2\Delta x^2}\right), C_7 = \left(\frac{9}{8} - \frac{3v\Delta t}{4\Delta x} - \frac{k\Delta t}{\Delta x^2}\right), C8 = \left(\frac{k\Delta t}{2\Delta x^2}\right)$

3.1. Formulation for boundary nodes

The boundary nodes $1, 2$ and right boundary node n needs special formulation for the approximation of variable. We have adjusted imaginary nodes at left and right side at distance of $\frac{\Delta x}{2}$ out of domain boundary as indicated in below Figure 2, Values of variable at these imaginary or mirror nodes can be approximated as,

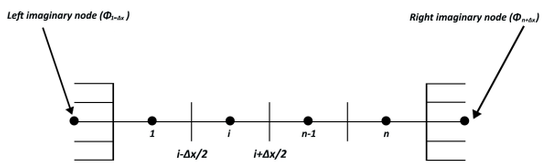

Figure 4: Adjustment of left and right imaginary node .

$$\phi_L = \frac{\phi_1 + \phi_{1-\Delta x}}{2} \tag{16}$$

$$\phi_R = \frac{\phi_n + \phi_{n+\Delta x}}{2} \tag{17}$$

Equation (16) and (17) have been put in the below approximation of Left and Right imaginary node respectively as:

$$\phi_{1-\Delta x} = \phi_0 = 2\phi_L - \phi_1 \tag{18}$$

This Equation (18) has shown the approximation at left imaginary node where ϕ_L represents the Variable at left boundary of computational domain.

$$\phi_{n+\Delta x} = 2\phi_R - \phi_n \tag{19}$$

This Equation (19) has indicated the approximation at Left imaginary node where ϕ_R represents the Variable at right boundary of computational domain. Now for node 1 the variable at west face $\phi_{1-\frac{\Delta x}{2}}$ is known, because its west face coincides with the physical boundary of the domain,

$$\phi_{1-\frac{\Delta x}{2}} = \phi_L. \tag{20}$$

As the major advantage of finite volume method is its ability to ensure the law of conservation. In the finite volume formulation for a common interface of adjacent control volumes, we have same expression for the variable approximation. In this way east interface of node 1 is the west interface for node 2 and for both nodes approximation at this common interface consistent i.e, substituting $i = 2$ into Equation (8), we have found the approximation at east interface of node 1 as:

$$\phi_{2-\frac{\Delta x}{2}} = \phi_{1+\frac{\Delta x}{2}} = -\frac{1}{8}\phi_0 + \frac{3}{4}\phi_1 + \frac{3}{8}\phi_2. \tag{21}$$

Here ϕ_0 is our left imaginary node. Substitute Equation (18) into (21), we have seen,

$$\phi_{2-\frac{\Delta x}{2}} = \phi_{1+\frac{\Delta x}{2}} = \frac{7}{8}\phi_1 + \frac{3}{8}\phi_2 - \frac{1}{4}\phi_L, \tag{22}$$

and the Gradient approximation at East and west interface of node 1 using Equation (8) and (9) given:

$$\left(\frac{\partial \phi}{\partial x}\right)_{1+\frac{\Delta x}{2}} = \left(\frac{\phi_2 - \phi_1}{\Delta x}\right) + O(\Delta x^2). \tag{23}$$

$$\left(\frac{\partial \phi}{\partial x}\right)_{1-\frac{\Delta x}{2}} = \left(\frac{\phi_1 - \phi_0}{\Delta x}\right) + O(\Delta x^2). \tag{24}$$

Using Equation (20),(22), (23), (24) and Equation (4) becomes,

$$\begin{aligned} & \frac{\Delta x}{2}\left(\frac{7}{8}\phi_{1,j+1} + \frac{3}{8}\phi_{2,j+1} + \frac{3}{4}\phi_{L,j+1}\right) - \frac{\Delta x}{2}\left(\frac{7}{8}\phi_{1,j} + \frac{3}{8}\phi_{2,j} + \frac{3}{4}\phi_{L,j}\right) \\ + \quad & v\int_j^{j+1}\left(\frac{7}{8}\phi_1 + \frac{3}{8}\phi_2 - \frac{5}{4}\phi_L\right)dt = k\int_j^{j+1}(\phi_0 - 2\phi_i + \phi_{i+1})\,dt. \end{aligned} \tag{25}$$

Here, we have substituted the value of left imaginary node ϕ_0, then after some simplification and applying θ scheme for $\theta = \frac{1}{2}$ for temporal approximation at each node we have justified the below discretized equation for node 1,

$$\begin{aligned} & \left(\frac{7}{16} + \frac{7v\Delta t}{16\Delta x} + \frac{3k\Delta t}{2\Delta x^2}\right)\phi_1^{j+1} + \left(\frac{3}{16} + \frac{3v\Delta t}{16\Delta x} - \frac{k\Delta t}{2\Delta x^2}\right)\phi_2^{j+1} \\ = \quad & \left(\frac{7}{16} - \frac{7v\Delta t}{16\Delta x} - \frac{3k\Delta t}{2\Delta x^2}\right)\phi_1^{j} + \left(\frac{3}{16} - \frac{3v\Delta t}{16\Delta x} + \frac{k\Delta t}{2\Delta x^2}\right)\phi_2^{j} \\ + \quad & \left(\frac{3}{8} + \frac{5v\Delta t}{8\Delta x} + \frac{k\Delta t}{\Delta x^2}\right)\phi_L^{j} + \left(-\frac{3}{8} + \frac{5v\Delta t}{8\Delta x} + \frac{k\Delta t}{\Delta x^2}\right)\phi_L^{j+1} \end{aligned} \tag{26}$$

This Equation (26) represents the Fully discretised equation for node 1. Now for node 2 the variable approximation at west interface is given in Equation (22). By substituting $i = 2$ Equation (4) gives the variable approximation at east interface of node 2,

$$\phi_{2+\frac{\Delta x}{2}} = \frac{3}{8}\phi_0 - \frac{5}{4}\phi_{1,j} + \frac{15}{8}\phi_{2,j}. \tag{27}$$

We have put approximate value of imaginary node ϕ_0 (see Equation (18) into Equation (27) then we have finalized,

$$\phi_{2+\frac{\Delta x}{2}} = -\frac{13}{8}\phi_1 + \frac{15}{8}\phi_2 + \frac{3}{4}\phi_L. \tag{28}$$

This Equation (28) represents the variable approximation at east interface of node 2. By substituting Equation (22), (28) and gradient approximations (see Equation (8) and Equation (9)) for $i = 2$ in semi- discretised Equation (4) we have got the below expression as,

$$\begin{aligned} & \frac{\Delta x}{2}\left(-\frac{3}{4}\phi_{1,j+1} + \frac{9}{4}\phi_{2,j+1} + \frac{1}{2}\phi_{L,j+1}\right) - \frac{\Delta x}{2}\left(-\frac{3}{4}\phi_{1,j} + \frac{9}{4}\phi_{2,j} + \frac{1}{2}\phi_{L,j}\right) \\ + \quad & v\int_j^{j+1}\left(-\frac{5}{2}\phi_1 + \frac{3}{2}\phi_2 + \phi_L\right)dt = k\int_j^{j+1}(\phi_1 - 2\phi_2 + \phi_3)\,dt. \end{aligned} \tag{29}$$

Here, we are divided the whole Equation (29) by *Deltax* and also applied θ scheme for $\theta = \frac{1}{2}$ to evaluate temporal integral over each node then it gives the result in the following form:

$$\begin{aligned} & \left(-\frac{3}{8} - \frac{5v\Delta t}{4\Delta x} - \frac{k\Delta t}{2\Delta x^2}\right)\phi_1^{j+1} + \left(\frac{9}{8} + \frac{3v\Delta t}{4\Delta x} + \frac{k\Delta t}{\Delta x^2}\right)\phi_2^{j+1} + \left(-\frac{k\Delta t}{2\Delta x^2}\right)\phi_3^{j+1} \\ = \quad & \left(-\frac{3}{8} + \frac{5v\Delta t}{4\Delta x} + \frac{k\Delta t}{2\Delta x^2}\right)\phi_1^{j} + \left(\frac{9}{8} - \frac{3v\Delta t}{4\Delta x} - \frac{k\Delta t}{\Delta x^2}\right)\phi_2^{j} + \left(\frac{k\Delta t}{2\Delta x^2}\right)\phi_3^{j} \\ + \quad & \left(\frac{1}{4} - \frac{v\Delta t}{2\Delta x}\right)\phi_L^{j} + \left(-\frac{1}{4} - \frac{v\Delta t}{2\Delta x}\right)\phi_L^{j+1} \end{aligned} \tag{30}$$

Equation (30) shows our fully discretized equation for node 2. For right boundary node M by taking $i = M$ from Equation (6) and Equation (7), we have put as the following approximations,

$$\phi_{M+\frac{\Delta x}{2}} = \frac{3}{8}\phi_{M-2} - \frac{5}{4}\phi_{M-1} + \frac{15}{8}\phi_M. \tag{31}$$

$$\phi_{M-\frac{\Delta x}{2},j} = -\frac{1}{8}\phi_{M-2} + \frac{3}{4}\phi_{M-1} + \frac{3}{8}\phi_M. \tag{32}$$

Equation (31) and Equation (32) have shown spatial approximation at east and west interface of node M respectively. For $i = M$ the gradient approximation (see Equation (8) and Equation (9)) becomes,

$$\left(\frac{\partial \phi}{\partial x}\right)_{M+\frac{\Delta x}{2}} = \left(\frac{\phi_{M+1} - \phi_M}{\Delta x}\right) + O(\Delta x^2). \tag{33}$$

$$\left(\frac{\partial \phi}{\partial x}\right)_{M-\frac{\Delta x}{2}} = \left(\frac{\phi_M - \phi_{M-1}}{\Delta x}\right) + O(\Delta x^2). \tag{34}$$

Equation (33) and Equation (34) represents the gradient approximation at east and west interface of node n respectively. Here ϕ_{M+1} is our right imaginary node approximate in (19). Now using interface approximations given in (31)-(34) our semi-discretized Equation 4 after dividing by Δx becomes,

$$\begin{aligned} & \frac{1}{2}\left(\frac{1}{4}\phi_{M-2,j+1} - \frac{1}{2}\phi_{M-1,j+1} + \frac{9}{4}\phi_{M,j+1}\right) - \frac{1}{2}\left(\frac{1}{4}\phi_{M-2,j} - \frac{1}{2}\phi_{M-1,j} + \frac{9}{4}\phi_{M,j}\right) \\ + \quad & \frac{v}{\Delta x}\int_j^{j+1}\left(\frac{1}{2}\phi_{M-2} - 2\phi_{M-1} + \frac{3}{2}\phi_M\right)dt = \frac{k}{\Delta x^2}\int_j^{j+1}(2\phi_R - 3\phi_M + \phi_{M-1})\,dt. \end{aligned} \tag{35}$$

Now by applying *theta* scheme for $\theta = \frac{1}{2}$ we get the below expression as,

$$\begin{aligned} & \left(\frac{1}{8} + \frac{v\Delta t}{4\Delta x}\right)\phi_{M-2}^{j+1} + \left(-\frac{1}{4} - \frac{v\Delta t}{\Delta x} - \frac{k\Delta t}{2\Delta x^2}\right)\phi_{M-1}^{j+1} + \left(\frac{9}{8} + \frac{3v\Delta t}{4\Delta x} + \frac{3k\Delta t}{2\Delta x^2}\right)\phi_M^{j+1} \\ = \quad & \left(\frac{1}{8} - \frac{v\Delta t}{4\Delta x}\right)\phi_{M-2}^{j} + \left(-\frac{1}{4} + \frac{v\Delta t}{\Delta x} + \frac{k\Delta t}{2\Delta x^2}\right)\phi_{M-1}^{j} + \left(\frac{9}{8} - \frac{3v\Delta t}{4\Delta x} - \frac{3k\Delta t}{2\Delta x^2}\right)\phi_M^{j} \\ + \quad & \left(\frac{k\Delta t}{\Delta x^2}\right)\phi_R^{j} + \left(\frac{k\Delta t}{\Delta x^2}\right)\phi_R^{j+1} \end{aligned} \tag{36}$$

This Equation (36) is our fully discretized equation for right boundary node M where ϕ_R represents the variable at the east interface of node M. ϕ_R is known because it coincides with the right boundary of physical domain.

4. Stability and Convergence Analysis

4.1. Stability

The most common and popular technique to find the stability region of a numerical scheme is the Von-Neumann stability analysis approach based on Fourier mode analysis. According to Von-Neumann for stability a numerical scheme requires, $|\xi| \leq 1$.

Theorem 4.1. *Let $\hat{\phi_{i,j}}$ be the numerical approximation of the exact solution $\phi_{i,j}$, then scheme 15 is unconditionally stable over a finite domain and $3 \leq i \leq M_x - 1, 1 \leq j \leq N - 1$.*

Proof 1. *In Fourier analysis the amplification factor of error is represented by $\eta_{i,j} = \xi^j e^{s\beta i\Delta x}$ where ξ is a time dependent variable, s represents $\sqrt{-1}$ and β is wave number with associate wavelength $\lambda = \frac{2\pi}{|\beta|}$. When we have seen this factor our scheme (15), then its error equation become:*

$$\begin{aligned} & C_1\xi^{j+1}e^{s\beta(i-2)\Delta x} + C_2\xi^{j+1}e^{s\beta(i-1)\Delta x} + C_3\xi^{j+1}e^{s\beta(i)\Delta x} + C_4\xi^{j+1}e^{s\beta(i+1)\Delta x} \\ = \quad & C_5\xi^{j}e^{s\beta(i-2)\Delta x} + C_6\xi^{j}e^{s\beta(i-1)\Delta x} + C_7\xi^{j}e^{s\beta i\Delta x} + C_8\xi^{j}e^{s\beta(i+1)\Delta x} \end{aligned} \tag{37}$$

$$\begin{aligned} & \xi^{j+1}\left(C_1e^{-s2\beta\Delta x} + C_2e^{-s\beta\Delta x} + C_3 + C_4e^{s\beta\Delta x}\right) \\ = \quad & \left(C_5e^{-s2\beta\Delta x} + C_6e^{-s\beta\Delta x} + C_7 + C_8e^{s\beta\Delta x}\right)\xi^{j} \end{aligned} \tag{38}$$

$$\begin{aligned} & \xi^{j+1}\left(C_1e^{-s\beta\Delta x} + C_2 + C_3e^{s\beta\Delta x} + C_4e^{s2\beta\Delta x}\right) \\ = \quad & \left(C_5e^{-s\beta\Delta x} + C_6 + C_7e^{s\beta\Delta x} + C_8e^{s2\beta\Delta x}\right)\xi^{j} \end{aligned} \tag{39}$$

$$\xi^{j+1} = \left(\frac{C_5 e^{-s\beta\Delta x} + C_6 + C_7 e^{s\beta\Delta x} + C_8 e^{s2\beta\Delta x}}{C_1 e^{-s\beta\Delta x} + C_2 + C_3 e^{s\beta\Delta x} + C_4 e^{s2\beta\Delta x}} \right) \xi^{j} \tag{40}$$

After some simplification, the formulation can be put as:

$$\xi^{+1} = \left(\frac{\alpha - \beta - \gamma}{\alpha + \beta + \gamma} \right) \xi^{j} \tag{41}$$

α, β and γ are complex numbers in below form where $s = \sqrt{-1}$ and,

$$\begin{aligned} \alpha &= \left(\frac{5}{4}\cos(\beta\Delta x) - \frac{1}{4} \right) + s\left(\sin(\beta\Delta x)\right) \\ ,\beta &= \frac{v\Delta t}{\Delta x}\left((\cos(\beta\Delta x) - 1) + s(\frac{1}{2}\sin(\beta\Delta x) \right) \\ \gamma &= \frac{k\Delta t}{\Delta x^2}\left(cos(\beta\Delta x)(\cos(\beta\Delta x) - 1) + s(1 - \cos(\beta\Delta x))\sin(\beta\Delta x)\right) \end{aligned} \tag{42}$$

$$|\xi^{j+1}| = |\frac{\alpha - \beta - \gamma}{\alpha + \beta + \gamma}\xi^{j}| = \frac{|\alpha - (\beta + \gamma)|}{|\alpha + (\beta + \gamma)|}|\xi^{j}| \tag{43}$$

As we have known for two complex numbers we have the inequality as,

$$|z_1 - z_2| \leq |z_1 + z_2|. \tag{44}$$

This implies,

$$|\alpha - (\beta + \gamma)| \leq |\alpha + (\beta + \gamma)| \tag{45}$$

Applying this inequality expression 43 becomes,

$$|\xi^{j+1}| = \frac{|\alpha - (\beta + \gamma)|}{|\alpha + (\beta + \gamma)|}|\xi^{j}| \leq \frac{|\alpha + (\beta + \gamma)|}{|\alpha + (\beta + \gamma)|}|\xi^{j}| = 1|\xi^{j}|, \tag{46}$$

and this gives $|\xi^{j}| \leq 1$, which mean the proposed numerical scheme is unconditionally stable for each value of Δx and Δt.

Theorem 4.2. *Let $\hat{\Phi}_{i,j}$ represents the exact solution of the governing problem (2), where as $\Phi_{i,j}$ be the solution by our numerical scheme (15), then for all $0 \leq j \leq N+1$, we have the estimates:*

$$\|\hat{\Phi}_{i,j} - \Phi_{i,j}\|_{\infty} \leq c(\Delta x^2 + \Delta t^2) \tag{47}$$

where, $\|\hat{\Phi}_{i,j} - \Phi_{i,j}\|_{\infty} = \max 1 \leq i \leq M_x |\hat{\Phi}_{i,j} - \Phi_{i,j}|, c$ is a positive constant which is independent of Δx and Δt where as $\|.\|$ stands for the discrete L^2 norm.

Proof 2. *Our numerical approximation gives an error $e_{i,j}$ at each grid point define as, $e_{i,j} = \hat{\Phi}_{i,j} - \Phi_{i,j}$ where, $e_i^j = (e_1^j, e_2^j, e_3^j, \cdots, e_M^j)$ and $e_i^0 = 0$, we have from our numerical scheme (15),*

if $j = 1$,

$$E_i^1 = \left(\frac{1}{8} + \frac{v\Delta t}{4\Delta x}\right)e_{i-2}^1 + \left(-\frac{1}{4} - \frac{v\Delta t}{\Delta x} - \frac{k\Delta t}{2\Delta x^2}\right)e_{i-1}^1 + \left(\frac{9}{8} + \frac{3v\Delta t}{4\Delta x} + \frac{k\Delta t}{\Delta x^2}\right)e_i^1 + \left(\frac{-k\Delta t}{2\Delta x^2}\right)e_{i+1}^1 \tag{48}$$

for $j > 1$,

$$E_i^j = \left(\frac{1}{8} + \frac{v\Delta t}{4\Delta x}\right)e_{i-2}^j + \left(-\frac{1}{4} - \frac{v\Delta t}{\Delta x} - \frac{k\Delta t}{2\Delta x^2}\right)e_{i-1}^j + \left(\frac{9}{8} + \frac{3v\Delta t}{4\Delta x} + \frac{k\Delta t}{\Delta x^2}\right)e_i^j + \left(\frac{-k\Delta t}{2\Delta x^2}\right)e_{i+1}^j \tag{49}$$

where $E_i^j \leq c(\Delta x^2 + \Delta t^2), i = 3, 4..., M-1, j = 0, 1, 2, 3, 4, ..., N+1$ and c is a positive constant which is independent of Δx and Δt.

We can use the mathematical induction to prove the Theorem 4.2. Let $j = 1$ and assume $|e_m^1| = \max 1 \leq i \leq M_x |e_i^1|$.

$$\begin{aligned} \|e_m^1\|_{\infty} = |e_m^1| &\leq \left(\tfrac{1}{8} + \tfrac{v\Delta t}{4\Delta x}\right)|e_{m-2}^1| + \left(-\tfrac{1}{4} - \tfrac{v\Delta t}{\Delta x} - \tfrac{k\Delta t}{2\Delta x^2}\right)|e_{m-1}^1| + \left(\tfrac{9}{8} + \tfrac{3v\Delta t}{4\Delta x} + \tfrac{k\Delta t}{\Delta x^2}\right)|e_m^1| + \left(\tfrac{-k\Delta t}{2\Delta x^2}\right)|e_{m+1}^1| \\ &\leq \left| \left(\tfrac{1}{8} + \tfrac{v\Delta t}{4\Delta x}\right)e_{m-2}^1 + \left(-\tfrac{1}{4} - \tfrac{v\Delta t}{\Delta x} - \tfrac{k\Delta t}{2\Delta x^2}\right)e_{m-1}^1 + \left(\tfrac{9}{8} + \tfrac{3v\Delta t}{4\Delta x} + \tfrac{k\Delta t}{\Delta x^2}\right)e_m^1 + \left(\tfrac{-k\Delta t}{2\Delta x^2}\right)e_{m+1}^1 \right| \\ &= |E_m^1| \leq c(\Delta x^2 + \Delta t^2) \end{aligned} \tag{50}$$

Suppose that if $j \leq n, \|e_i^n\|_{\infty} \leq c(\Delta x^2 + \Delta t^2)$ hold and assume $j = n+1$,let $|e_m^{n+1}| = \max 1 \leq i \leq M_x |e_i^{n+1}|$

$$\begin{aligned} \|e_m^{n+1}\|_{\infty} = |e_m^{n+1}| &\leq \left(\tfrac{1}{8} + \tfrac{v\Delta t}{4\Delta x}\right)|e_{m-2}^{n+1}| + \left(-\tfrac{1}{4} - \tfrac{v\Delta t}{\Delta x} - \tfrac{k\Delta t}{2\Delta x^2}\right)|e_{m-1}^{n+1}| + \left(\tfrac{9}{8} + \tfrac{3v\Delta t}{4\Delta x} + \tfrac{k\Delta t}{\Delta x^2}\right)|e_m^{n+1}| + \left(\tfrac{-k\Delta t}{2\Delta x^2}\right)|e_{m+1}^{n+1}| \\ &\leq \left| \left(\tfrac{1}{8} + \tfrac{v\Delta t}{4\Delta x}\right)e_{m-2}^{n+1} + \left(-\tfrac{1}{4} - \tfrac{v\Delta t}{\Delta x} - \tfrac{k\Delta t}{2\Delta x^2}\right)e_{m-1}^{n+1} + \left(\tfrac{9}{8} + \tfrac{3v\Delta t}{4\Delta x} + \tfrac{k\Delta t}{\Delta x^2}\right)e_m^{n+1} + \left(\tfrac{-k\Delta t}{2\Delta x^2}\right)e_{m+1}^{n+1} \right| \\ &= |E_m^{n+1}| \leq c(\Delta x^2 + \Delta t^2) \end{aligned} \tag{51}$$

which complete the proof .

5. Numerical simulation

Example-1

Let $\phi(x,t)$ be the our physical property transported by means of convection and diffusion process through one dimensional domain. Analytical solution of the problem is given [57] by $\phi(x,t)$= $\frac{1}{\sqrt{t+1}}e^{(-(x-v(t+1))^2)/4k(t+1)}$ is considered on the finite domain $[0,1]\times[0,1]$. The initial and boundary values are calculated from exact solution by taking $t=0$ and $x=0, x=1$, respectively.

For time step $\Delta t = 1/1000$ and spatial step size $\Delta x = 1/360$ convection diffusion problem is solved using our proposed numerical form of finite volume method. Our aim in this numerical example is to observe the performance of our numerical scheme for convection dominant phenomenons, in this regard we have considered the below two cases for convection dominancy as,

1) $k = 0.009$ and $v = 1.5$

2) $k = 0.02$ and $v = 2$.

obtain numerical solution and maximum error for each case are shown below, The magnitude of maximum error

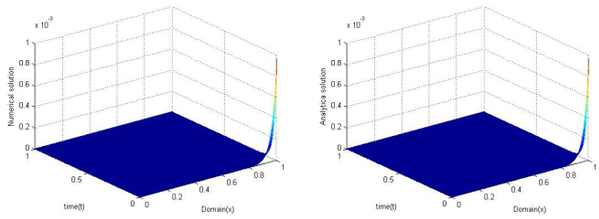

Figure 5: Numerical(Left) and analytical(Right) solution produced by proposed finite volume method for case-1.

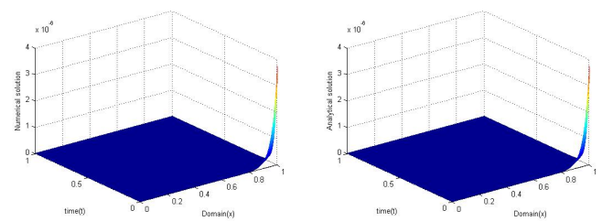

Figure 6: Numerical(Left) and analytical(Right) solution produced by proposed finite volume method for case-2.

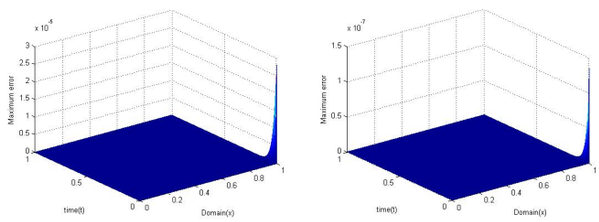

Figure 7: Maximum error for case-1(left) and case-2(right) produced by proposed finite volume method.

produced by our numerical approach for case-1 and case-2 is 2.7880×10^{-05} and 1.3441×10^{-07} respectively. As our formulation based on upwind approach to deal the Convection dominancy which is measured by Peclet number ($Pe=\frac{\Delta x v}{k}$). Above case-1 and case-2 both shows convection dominancy, numerical results obtained for both cases are graphically represented in below Figure 8

Figure 5– Figure 8 indicates that, numerical results obtained by our newly constructed numerical scheme for both Convection dominant cases are highly accurate and consistent with analytical solution of the problem. The spatial and temporal convergence order of the newly developed numerical scheme for a convection dominant case $(k=0.08, v=1)$ displayed in Table 1 and Table 2 respectively. In Table 1 spatial convergence order has been proved taking spatial step size (Δx) as $\frac{1}{15}, \frac{1}{30}, \frac{1}{60}$ and $\frac{1}{120}$, where as the time level is fixed at $\frac{1}{400}$, $\frac{1}{800}$ and $\frac{1}{1200}$. For convection dominancy results of temporal convergence order are displayed in Table 2. These results of temporal convergence obtained by considering temporal step size (Δt) as $\frac{1}{15}, \frac{1}{30}, \frac{1}{60}$ and $\frac{1}{120}$, where as spatial step size is fixed as $\frac{1}{400}, \frac{1}{800}$ and $\frac{1}{1200}$.

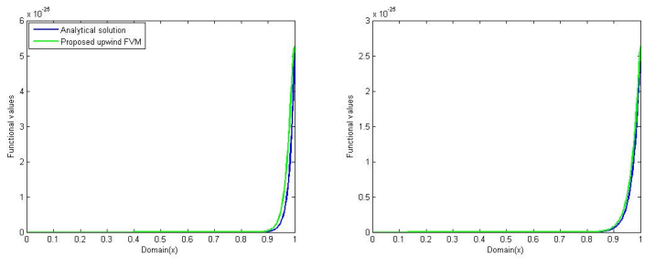

Figure 8: Graphical representation of analytical and numerical solution for case-1(left) and case-2(right) respectively.

Table 1: Spatial convergence order for convection dominancy taking $(k = 0.08, v = 1)$

	$\Delta t = 1/400$		$\Delta t = 1/800$		$\Delta t = 1/1200$	
Δx	**Max-Error**	**Order**	**Max-Error**	**Order**	**Max-Error**	**Order**
1/15	0.0047	–	0.0047	–	0.0047	–
1/30	0.0013	1.9777	0.0013	1.9775	0.0013	1.9774
1/60	3.5479×10^{-4}	1.9208	3.5507×10^{-4}	1.9200	3.5512×10^{-4}	1.9199
1/120	9.0667×10^{-5}	1.9683	9.0937×10^{-5}	1.9652	9.088×10^{-5}	1.9646

Table 2: Temporal convergence order convection dominancy taking $(k = 0.08, v = 1)$

	$\Delta x = 1/400$		$\Delta x = 1/800$		$\Delta x = 1/1200$	
Δt	**Max-Error**	**Order**	**Max-Error**	**Order**	**Max-Error**	**Order**
1/15	3.4053×10^{-4}	–	3.4086×10^{-4}	–	3.4092×10^{-4}	–
1/30	8.4506×10^{-5}	2.0106	8.4785×10^{-5}	2.0073	8.4837×10^{-5}	2.0067
1/60	2.0808×10^{-5}	2.0219	2.1086×10^{-5}	2.0075	2.1140×10^{-5}	2.0047
1/120	4.9330×10^{-6}	2.0766	5.3014×10^{-6}	2.0193	5.2539×10^{-6}	2.0086

Table 3: Spatial convergence order for convection dominancy taking $(k = 0.3, v = 2)$

	$\Delta t = 1/400$		$\Delta t = 1/800$		$\Delta t = 1/1200$	
Δx	**Max-Error**	**Order**	**Max-Error**	**Order**	**Max-Error**	**Order**
1/15	3.6898×10^{-4}	–	3.6928×10^{-4}	–	3.6934×10^{-4}	–
1/30	9.4064×10^{-5}	1.9718	9.4363×10^{-5}	1.9684	9.4419×10^{-5}	1.9678
1/60	2.3192×10^{-5}	2.0200	2.3487×10^{-5}	2.0064	2.3542×10^{-5}	2.0039
1/120	6.5800×10^{-6}	1.8175	5.8672×10^{-6}	2.0011	5.8308×10^{-6}	2.0134

Table 4: Temporal convergence order for convection dominancy $(k = 0.3, v = 2)$

	$\Delta x = 1/400$		$\Delta x = 1/800$		$\Delta x = 1/1200$	
Δt	**Max-Error**	**Order**	**Max-Error**	**Order**	**Max-Error**	**Order**
1/15	0.4053×10^{-4}	–	3.4086×10^{-4}	–	3.4092×10^{-4}	–
1/30	8.4506×10^{-5}	2.0106	8.4785×10^{-5}	2.0076	8.4837×10^{-5}	2.0067
1/60	2.0808×10^{-5}	2.0219	2.1086×10^{-5}	2.0075	2.1140×10^{-5}	2.0047
1/120	4.9330×10^{-6}	2.0766	5.2014×10^{-6}	2.0193	5.2539×10^{-6}	2.0086

With same process, results of spatial and temporal convergence order of our proposed method for another convection dominant case $(k = 0.3, v = 2)$ are displayed in below Table 3 and Table 4 respectively. For spatial convergence in Table 3 spatial step size (Δx) as $\frac{1}{15}, \frac{1}{30}, \frac{1}{60}$ and $\frac{1}{120}$, where as the time level is fixed at $\frac{1}{400}$, $\frac{1}{800}$ and $\frac{1}{1200}$.

Table 4 shows the results of temporal convergence order for c of convection dominancy $(k = 0.3, v = 2)$. To proof the temporal convergence order, the temporal step size (Δt) has been taken as, $\frac{1}{15}, \frac{1}{30}, \frac{1}{60}$ and $\frac{1}{120}$, where as spatial step size is fixed as $\frac{1}{400}, \frac{1}{800}$ and $\frac{1}{1200}$.

The obtained spatial and temporal convergence order displayed in Table 1 -Table 4 for both convection dominant

cases, supports to theoretical approach of newly developed algorithm about the spatial and temporal convergence order.

Example-2

The analytical solution of the one-dimensional unsteady convection-diffusion of a Gaussian pulse of unit height, centred at $x = 1$ in a bounded region is given in[25] is, $\phi(x,t)= \frac{1}{\sqrt{4t+1}} e^{(-(x-1-vt))^2)/k(4t+1)}$. The initial and boundary values are calculated from exact solution by taking $t = 0$ and $x = 0, x = 1$, respectively. $\phi(x,t)$ is the physical property transported by means of convection and diffusion process through one dimensional domain. For time step $\Delta t = 1/1000$ and spatial step size $\Delta x = 1/360$ convection diffusion problem is solved using our proposed numerical form of finite volume method over finite computational domain $[0,1] \times [0,1]$.

Here we have considered two convection dominant cases as,

1) $k = 0.01$ and $v = 5$

2) $k = 0.005$ and $v = 5$.

The purpose of solving this numerical example is, to compare the numerical results of our proposed upwind approach with most popular and commonly used (central differencing form of finite volume method) numerical form of finite volume method[10, 11, 12, 13]. Obtained numerical solution and maximum error produced by both numerical scheme are listed below, For case-1 of convection dominancy, numerical results of our proposed approach and central

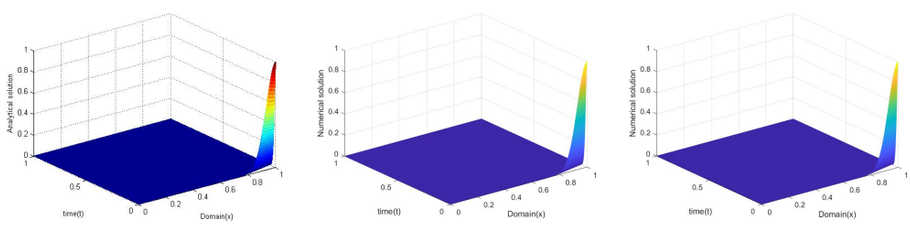

Figure 9: Analytical(Left) and numerical solution produced by our proposed approach(Mid) and Central differencing approach(Right) .

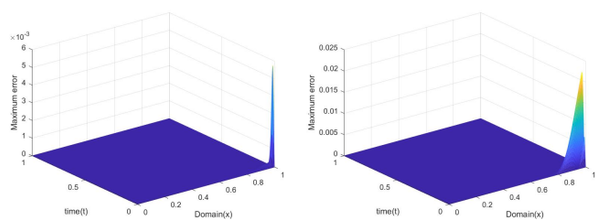

Figure 10: Maximum error produced by our upwind approach $(Left)$ and Central differencing approach $(Right)$ for case-1 are represented.

differencing approach are shown in Figure 9. Where as, Figure 10 represents the Maximum error of both numerical schemes. For case-1 of convection dominancy, magnitude of maximum error produced by proposed upwind approach and central differencing approach are respectively as 0.0057 and 0.0222.

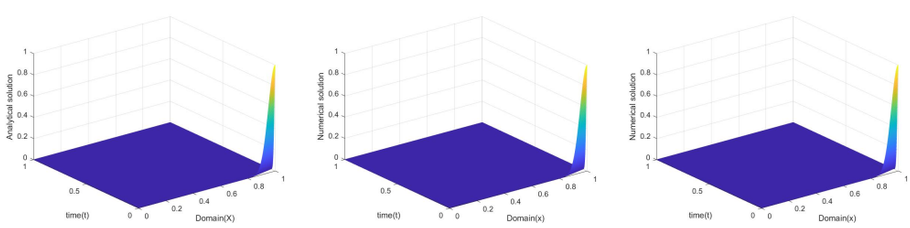

Figure 11: Analytical(Left) and numerical solution produced by our proposed approach(Mid) and Central differencing approach(Right).

For case-2 of convection dominancy, numerical results of our proposed approach and central differencing approach are shown in Figure 11. Figure 12 represents the Maximum error of both numerical schemes. For case-2 of convection dominancy, magnitude of maximum error produced by proposed upwind approach and central differencing approach are respectively as 0.0051 and 0.0427. Figure 13 shows a comparison of modified upwind approach and central differencing form of finite volume method for Peclet number(Pe)0.1667 (Figure at Left) and $Pe = 0.3733$ (Figure at right). From Figure 13 it is clear that, for both convection dominant flow cases, approximation by modified upwind approach is close to exact solution. As we observed that, while approximation the problem in both convection dominant

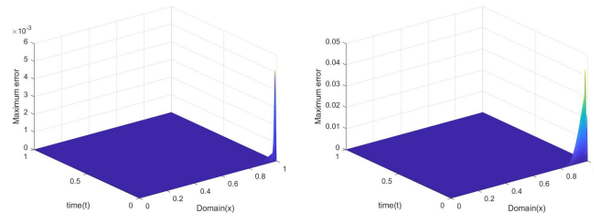

Figure 12: Maximum error produced by our upwind approach $(Left)$ and Central differencing approach $(Right)$ for case-2 are represented.

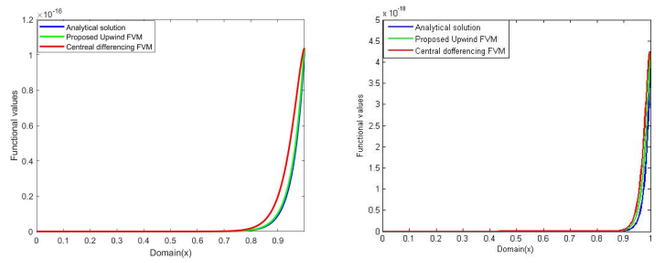

Figure 13: Graphical comparison of numerical results produced by modified approach and central differencing form for $Pe = 0.1667$ and $pe = 0.3733$.

cases, our proposed method give results with less maximum error. This indicates that, approximation of problem using modified upwind approach is more close to exact solution as compare to central differencing one. Also, the graphical comparison in Figure 12 illustrate that, for both values of Peclet number(Pe) approximation of newly constructed numerical approach are highly accurate and close to exact solution.

Remark 1. *While approximating convective terms at spatial interfaces, the central differencing finite volume method ignore the convection dominancy or flow direction. This numerical approach gives equal weight to neighbour nodes of interface taking their mean value for the approximation of variable at spatial interface. The approximation of convective terms by central differencing form of finite volume method at east and wets interface are respectively given as,* $\phi_{i+\frac{\Delta x}{2}} = \frac{\phi_i+\phi_{i+1}}{2}, \phi_{i-\frac{\Delta x}{2}} = \frac{\phi_i+\phi_{i-1}}{2}$.

Example-3

Let $\phi(x,t)$ represent the physical property of temperature which is transported by means of convection and diffusion process through one dimensional domain $[0,1]\times[0,1]$. Analytical solution of the problem is $\phi(x,t) = sin(\pi x)e^{(-(x-1-vt))^2)/4k(t+1)}$. Boundary conditions are homogenous Dirichelt type, the initial and boundary values are calculated from exact solution by taking $t = 0$ and $x = 0, x = 1$, respectively.

Our main focus in this numerical example is to study the physical phenomena of heat flow and temperature distribution inside a one dimensional rod (see Figure 13). The boundaries of road are insulated and there is no heat source or sink in rod. The physical length (L) of the rod represents our one dimensional computational domain and 0^0 temperature is fixed at the both ends of rod. Our proposed upwind form of finite volume method is used for the numerical approximation of temperature inside the rod. Taking different values of convective velocity (V) and diffusion coefficient (k) results effect of convection and diffusion have been analysed.

Figure 14: One dimensional insulated rod of length L.

As the rod is insulated so there is no heat flow across the boundary of the rod and also there is no heat source inside the rod. The initial temperature of the road should go down with the passage of time and finally there will be a uniform temperature in whole rod.

In Figure 15 Figures from left to right shows the profile of temperature distribution inside thin rod for $v = 1$,

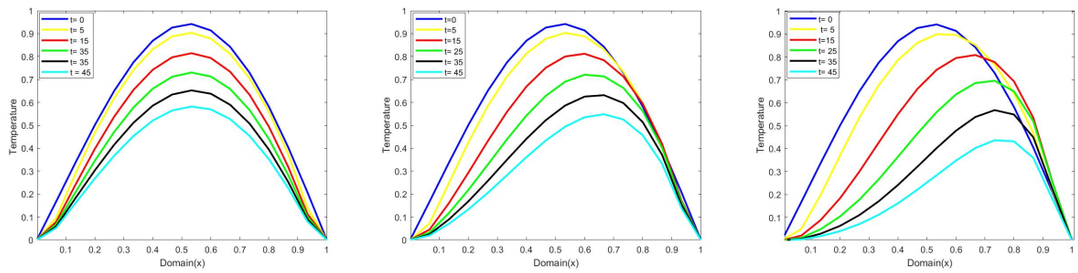

Figure 15: Temperature distribution at different time levels with fixed $k = 1$ taking $v = 1$(left fig),$v = 5$(middle fig) and $v = 10$(right fig).

$v = 5$ and $v = 10$ where as the value of diffusion coefficient is fixed $(K = 1)$. In Figure 15 left figure, show the fall of temperature in a symmetric pattern, and this symmetrical distribution of temperature is due to the same rate of convection and diffusion process $(v = k = 1)$.

Where as middle figure and figure at right, show the physical phenomena of temperature distribution for convection dominancy taking $v = 5$ and $v = 10$ respectively with fixed $k = 1$. Middle figure and right side figure, show the effect of convective velocity v, these both figures indicates that, for high convective velocity the is the graph is pushed in the direction of velocity or flow direction.

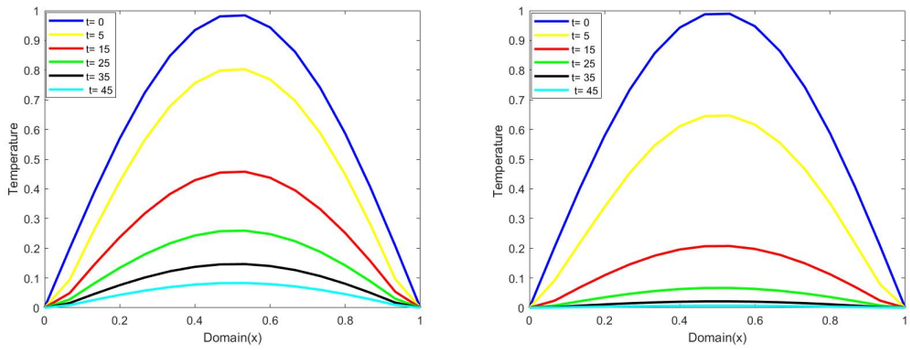

Figure 16: Temperature distribution at nodal point at different time levels with fixed $v = 1$ taking $k = 5$(left fig) and $k = 10$(right fig).

In Figure16 figure at left ant figure at right, shows the profile of temperature distribution with diffusion dominancy inside thin rod for $k = 5$ and $k = 10$ respectively, where as the value of convective velocity is fixed $(v = 1)$.

In Figure 16 both figures represents that, diffusion dominancy ensure the symmetrical profile of temperature distribution at each time level. From these both figures it is clear that, for high value of diffusion coefficient (k) temperature decreases fastly.

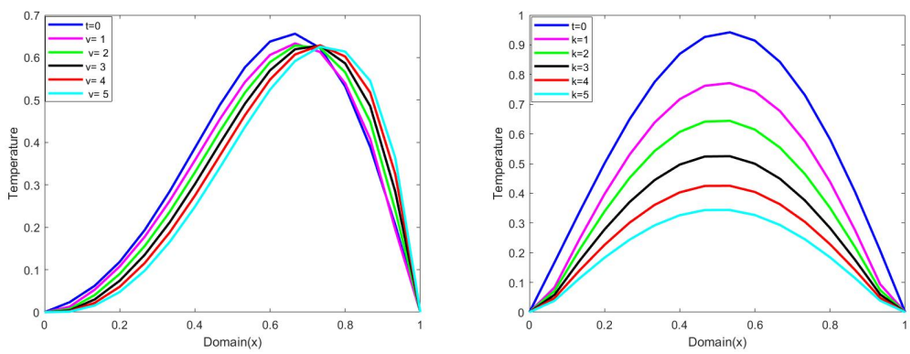

Figure 17: Temperature profile at fixed time level $t = 20^{th}$ for fixed $k = 0.1$(left fig) and $v = 0.1$(right fig).

Figure 17 illustrates the effect of convective velocity(v)(Left figure) and diffusion dominancy(figure at right) at a fixed time level $(t = 20^{th})$. Taking a fixed value of diffusion coefficient $k = 0.1$ with different values for $v = 1,2,3,4,5$ the effect of convective velocity is investigated see Figure 17(Left). Figure 17(Rigt) explains the effect of diffusion dominancy taking diffusion coefficient $k = 1,2,3,4,5$ where as coefficient of convective velocity $v = 0.1$ is fixed at time level $(t = 20^{th})$.

Figure 17 indicates that, at fixed time level and fixed diffusion coefficient for high value of v the temperature

distribution profile is highly pushed along the direction of convective velocity. But, for fixed at fixed time level , for a fixed value of convective velocity V, as we increase the value of k, then the diffusion rate will be high and temperature will fastly go down. Due to this reason, there is fall of temperature profile in Figure 17(right) as we increase the value of k.

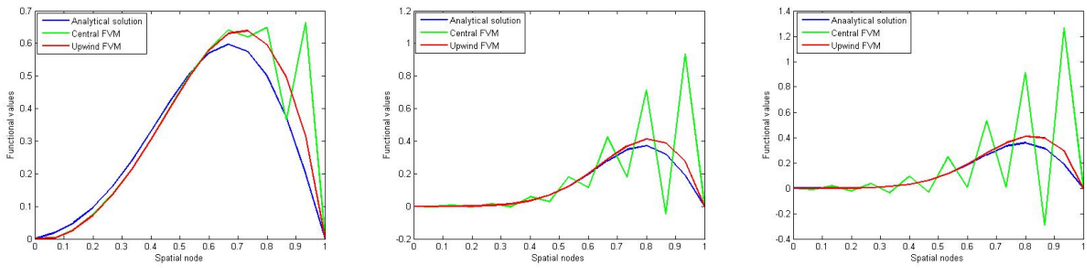

Figure 18: Comparison of modified Upwind FVM and Central differencing form of FVM for different values of Peclet number (Pe).

As the major weakness of central differencing finite volume method is that, this scheme cant treat the convection dominant phenomena. In this regard our proposed Upwind approach most suitable for the numerical approximation of such convection dominant phenomena. Figure 17 represents the comparison of formulated upwind approach and central differencing approach of finite volume method. Results obtained by both numerical schemes are mention for Peclet number $(Pe) = 4, 8.8889$ and 11.1111 are mentioned in Figure 17 form left to right respectively. Obtained results indicates that, the approximation by upwind finite volume method is more consistent with analytical solution but the central differencing approach of finite volume method gives highly disturbed solution for high values of peclet number (Pe). Example-4

Let $\phi(x,t)$ represent the physical property of which is transported by means of convection and diffusion process through one dimensional domain $[0,1]\times[0,1]$. Analytical solution of the problem is $\phi(x,t)$= $\frac{1}{\sqrt{t+20}} e^{(-(x-0.01-vt))^2)/4k(t+20)}$. Boundary conditions are non-homogenous Dirichelt type, the initial and boundary values are calculated from exact solution by taking $t = 0$ and $x = 0, x = 1$, respectively. In this numerical experiment, our aim is to analysis the distribution of functional values in one dimensional domain $[0,1]\times[0,1]$. The numerical approximation is done by our proposed upwind approach finite volume method and central differencing finite volume method.

As our developed algorithm is for convection dominancy, so we have performed this numerical experiment for different values of Peclet number $Pe = 5$ and $Pe = 10$. For each value of Pe numerical results obtained at different time levels $t = 10, t = 50$ and $t = 100$ are illustrated as, In Table 5,Table 6 and Table 7 numerical results for $Pe = 5$

Table 5: Comparative results of temperature distribution along axial direction when for Peclet number $Pe = 5$ and $t = 10$

Axial Distance(x)	0	0.1	0.2	0.3	0.4	0.5	0.6	0.7	0.8	0.9	1
Analytical solution	0.2235	0.2232	0.2215	0.2184	0.2141	0.2085	0.2018	0.1941	0.1856	0.1763	0.1664
Proposed Upwind FVM	0.2235	0.2233	0.2216	0.2185	0.2141	0.2085	0.2018	0.1942	0.1856	0.1760	0.1664
Central differencing FVM[10, 11, 12]	0.2235	0.2235	0.2214	0.2185	0.2139	0.2089	0.2012	0.1953	0.1837	0.1793	0.1664

Table 6: Comparative results of temperature distribution along axial direction when for Peclet number $Pe = 5$ and $t = 50$

Axial Distance(x)	0	0.1	0.2	0.3	0.4	0.5	0.6	0.7	0.8	0.9	1
Analytical solution	0.2225	0.2233	0.2227	0.2208	0.2175	0.2129	0.2071	0.2002	0.1924	0.1837	0.1743
Proposed Upwind FVM	0.2225	0.2231	0.2228	0.2209	0.2176	0.2129	0.2071	0.2003	0.1924	0.1829	0.1743
Central differencing FVM[10, 11, 12]	0.2225	0.2232	0.2229	0.2209	0.2173	0.2131	0.2066	0.2014	0.1897	0.1893	0.1743

are shown at time level $t = 10, t = 50$ and $t = 100$ respectively. From these results, it is clear that, solution obtained by our proposed upwind approach is highly close to exact solution at each time level. But the numerical solution of

Table 7: Comparative results of temperature distribution along axial direction when for Peclet number $Pe = 5$ and $t = 100$

Axial Distance(x)	0	0.1	0.2	0.3	0.4	0.5	0.6	0.7	0.8	0.9	1
Analytical solution	0.2201	0.22322	0.2231	0.2225	0.2205	0.2172	0.2126	0.2069	0.2000	0.1922	0.1835
Proposed Upwind FVM	0.2201	0.2214	0.2227	0.2225	0.2206	0.2174	0.2128	0.2070	0.2000	0.1914	0.1835
Central differencing FVM[10, 11, 12]	0.2201	0.2215	0.2228	0.2226	0.2205	0.2174	0.2121	0.2080	0.1974	0.1982	0.1835

central differencing FVM is showing the deviation from the exact result.

From Left to right Figure 19 shows the graphical representation of results shown in Table 5, Table 6 and Table 7 respectively.

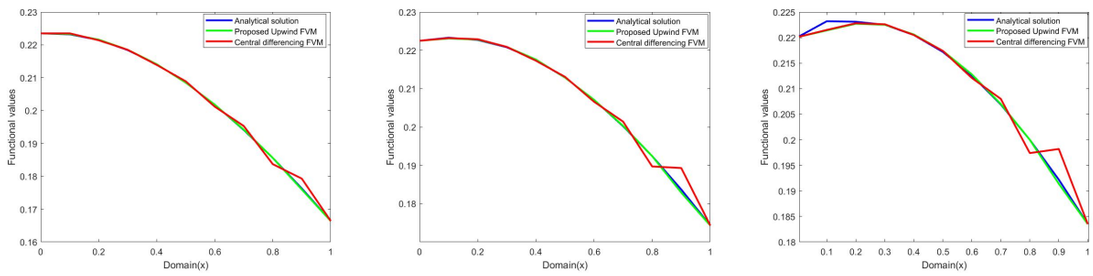

Figure 19: Comparison of modified Upwind FVM and Central differencing form of FVM for different values of Peclet number (Pe).

Table 8: Comparative results of temperature distribution along axial direction when for Peclet number $Pe = 10$ and $t = 10$

Axial Distance(x)	0	0.1	0.2	0.3	0.4	0.5	0.6	0.7	0.8	0.9	1
Analytical solution	0.2234	0.2234	0.2219	0.2191	0.2150	0.2096	0.2031	0.1956	0.1872	0.1780	0.1682
Proposed Upwind FVM	0.2234	0.2235	0.2220	0.2191	0.2150	0.2096	0.2031	0.1956	0.1872	0.1778	0.1682
Central differencing FVM[10, 11, 12]	0.2234	0.2242	0.2211	0.2203	0.2132	0.2122	0.1994	0.2009	0.1798	0.1884	0.1682

Table 9: Comparative results of temperature distribution along axial direction when for Peclet number $Pe = 10$ and $t = 50$

Axial Distance(x)	0	0.1	0.2	0.3	0.4	0.5	0.6	0.7	0.8	0.9	1
Analytical solution	0.2204	0.2226	0.2233	0.2227	0.2207	0.2174	0.2128	0.2070	0.2001	0.1922	0.1835
Proposed Upwind FVM	0.2204	0.2217	0.2230	0.2227	0.2209	0.2176	0.2129	0.2071	0.2001	0.1918	0.1835
Central differencing FVM[10, 11, 12]	0.2204	0.2223	0.2221	0.2242	0.2186	0.2206	0.2078	0.2143	0.1891	0.2086	0.1835

Table 10: Comparative results of temperature distribution along axial direction when for Peclet number $Pe = 10$ and $t = 100$

Axial Distance(x)	0	0.1	0.2	0.3	0.4	0.5	0.6	0.7	0.8	0.9	1
Analytical solution	0.2119	0.2167	0.2201	0.2223	0.2231	0.2224	0.2205	0.2171	0.2125	0.2068	0.1999
Proposed Upwind FVM	0.2119	0.2145	0.2185	0.2213	0.2226	0.2224	0.2206	0.2174	0.2128	0.2065	0.1999
Central differencing FVM[10, 11, 12]	0.2119	0.2150	0.2178	0.2224	0.2210	0.2249	0.2167	0.2229	0.2037	0.2199	0.1999

In Table 8,Table 9 and Table 10 numerical results for $Pe = 10$ are shown at time level $t = 10, t = 50$ and $t = 100$ respectively. Numerical results mentioned in these tables indicates that, numerical approximation of convection dominant problem by our proposed upwind approach is near to exact solution at each time level. But the numerical solution of central differencing FVM is showing the high difference from the exact solution.

From Left to right Figure 20 shows the graphical representation of results shown in Table 8, Table 9 and Table 10 respectively.

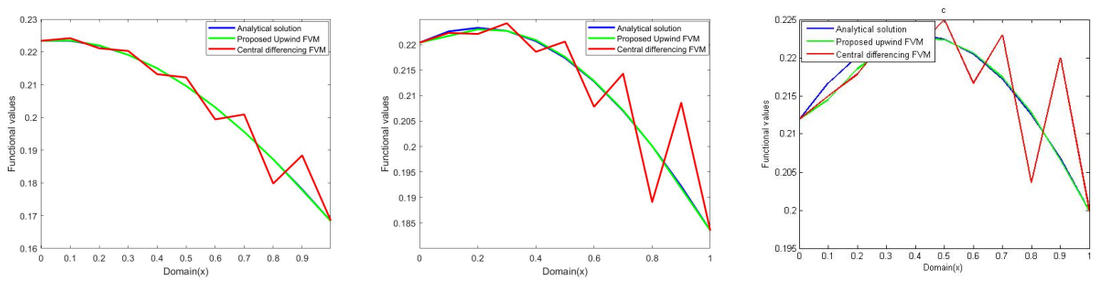

Figure 20: Comparison of modified Upwind FVM and Central differencing form of FVM for different values of Peclet number (Pe).

6. Conclusion

In this article, using Lagrange interpolation, new expressions obtained for spatial interface approximation of variable. Subsequently using these new interface approximations a numerical scheme based on upwind approach of finite volume method is constructed. This newly developed scheme gives second order accuracy in space and time with unconditional stability. This modified upwind approach is applied to addressed the convection-diffusion model numerically in convection dominant situations. The effect of convective velocity coefficient (v) and diffusion coefficient during the temperature distribution in a one dimensional rod is analysed. High value of convective velocity, temperature distribution profile is stretched in the direction of convective velocity. But for high value of diffusion coefficient (k) grow up, this implies that, for high rate of diffusion temperature at any fixed time level should be high. For the numerical approximation of convection dominant phenomena, taking different values of Peclet number (Pe) we have compared numerical results of our proposed upwind numerical approach and central differencing approach of finite volume method. These results show that, the proposed numerical approach is efficient and stable to approximate convection dominant problems, whereas the conventional finite volume method gives numerical un-stable results with non-physical oscillations.

References

[1] S.Karaa. A high-order compact ADI method for solving three-dimensional unsteady convection-diffusion problems, *Numerical Methods for Partial Differential Equations: An International Journal*,**2006**,*22*,983–993.

[2] W.j.Golz and J.R Dorroh.The convection-diffusion equation for a finite domain with time varying boundaries,*Applied mathematics letters*,**2001***14*,983–988.

[3] D.You. A high-order Padé ADI method for unsteady convection–diffusion equations,*Journal of Computational Physics*,**2006**,*214*,1–11.

[4] A.Chertock,A.Kurganov and G.Petrova.Fast explicit operator splitting method for convection–diffusion equations,*International journal for numerical methods in fluids*,**2009**,*59*,309–332.

[5] L.Zhu, G.Yuan and Q.Du. An efficient explicit/implicit domain decomposition method for convection-diffusion equations,*Numerical Methods for Partial Differential Equations: An International Journal*,**2010**,*26*,852–873.

[6] M.Dehghan. On the numerical solution of the one-dimensional convection-diffusion equation,*Mathematical Problems in Engineering*,**2005**,*2005*,61–74.

[7] R.Mohammadi.Exponential B-spline solution of convection-diffusion equations,*Applied Mathematics*,**2013**,*4*,933–944.

[8] H.Gomez,I.Colominas,F.Navarrina and M.Casteleiro. A hyperbolic model for convection-diffusion transport problems in CFD: Numerical analysis and applications,*RACSAM-Revista de la Real Academia de Ciencias Exactas, Fisicas y Naturales. Serie A. Matematicas*,**2008**,*102*319–334.

[9] A.Compte and R. Metzler.The generalized Cattaneo equation for the description of anomalous transport processes,*Journal of Physics A: Mathematical and General*,**1997**, *30*,7277-7289.

[10] A.Shukla,A.K.Singh,P. Singh,A. Shukla,A.K.Singh and P.A.Singh. comparative study of finite volume method and finite difference method for convection-diffusion problem,*American Journal of Computational and Applied Mathematics*,**2011**,*1*,67–73.

[11] R.Liu,D. Wang,X.Zhang,W.Li and B.Yu. Comparison Study on the Performances of Finite Volume Method and Finite Difference Method,*J. Appl. Math.*, **2013**,*2013*

[12] G.G.Botte,J.A. Ritter and R.E. White. Comparison of finite difference and control volume methods for solving differential equations,*Computers and Chemical Engineering* ,**2000**,*24*,2633–2654.

[13] B.P.Leonard. Comparison of truncation error of finite-difference and finite-volume formulations of convection terms,*Applied mathematical modelling*,**1994**,*18*,46–50.

[14] Kadalbajoo,K. Mohan and A. Awasthi. The Midpoint Upwind Finite Difference Scheme for Time-Dependent Singularly Perturbed Convection-Diffusion Equations on Non-Uniform Mesh, *International Journal for Computational Methods in Engineering Science and Mechanics*,**2011**,*12*,150–159.

[15] C.Varanasi,J.Y. Murthy and S. Mathur. Numerical schemes for the convection-diffusion equation using a meshless finite-difference method,*Numerical Heat Transfer, Part B: Fundamentals*,**2012**, *62*,1–27.

[16] G.F.Gromyko. A Finite-Difference Method for Nonstationary Convection–Diffusion Problems,*Differential Equations*,**2001**, *37*,961–969.

[17] J.Srinivasan and N.S. Rao. Numerical study of heat transfer in laminar film boiling by the finite-difference method,*International journal of heat and mass transfer*,**1984**, *27*,77–84.

[18] J.Zhang and D. Yang. Parallel characteristic finite difference method for convection–diffusion equations*Numerical methods for partial differential equations*,**2011**,*27*,854–866

[19] M.Gaultier,M.Lezaun and F.Vadillo.A problem of heat and mass transfer: proof of the existence condition by a finite difference method,*International journal for numerical methods in fluids*,**1993**,*16*,87–104.

[20] H.Sun and J.Zhang. A high-order finite difference discretization strategy based on extrapolation for convection diffusion equations, *Numerical Methods for Partial Differential Equations: An International Journal*, **2004**,*20*,18–32.

[21] Y.Shapira. Adequacy of finite difference schemes for convection-diffusion equations,*Numerical Methods for Partial Differential Equations*,**2002**,*18*,280–295.

[22] I.Noor,H. Syafutra and F.Ahmad.Simulation of heat transfer in cylinder husks furnace with finite difference method,*IOP Conference Series: Earth and Environmental Science*,**2016**,*31*.

[23] W.Liao. A compact high-order finite difference method for unsteady convection-diffusion equation,*International Journal for Computational Methods in Engineering Science and Mechanics*,**2012**,*13*,135–145.

[24] J.Zhang. Accelerated multigrid high accuracy solution of the convection-diffusion equation with high Reynolds number,*Numerical Methods for Partial Differential Equations: An International Journal*,**1997**,*13*,77–92.

[25] H.Karahan.Solution of weighted finite difference techniques with the advection–diffusion equation using spreadsheets,*Computer Applications in Engineering Education*,**2008**,*16*,147–156.

[26] E.Mitsoulis and J. Vlachopoulos.The finite element method for flow and heat transfer analysis,*Advances in Polymer Technology: Journal of the Polymer Processing Institute*,**1984**,*4*,107–121.

[27] B.L.Wang and Y.W. Mai.Transient one-dimensional heat conduction problems solved by finite element,*International Journal of Mechanical Sciences*,**2005**,*47*,303–317.

[28] S.Franz and T.LinB. Super convergence analysis of the Galerkin FEM for a singularly perturbed convection–diffusion problem with characteristic layers,*Numerical Methods for Partial Differential Equations: An International Journal*,**2008**,*24*,144–164.

[29] G.R.Richter. An explicit finite element method for convection-dominated steady state convection-diffusion equation,*SIAM journal on numerical analysis*,**1991**,*28*,744–759.

[30] X.Li,W. Wu and O.C Zienkiewicz. Implicit characteristic Galerkin method for convection–diffusion equations,*International Journal for Numerical Methods in Engineering*,**2000**,*47*,1689–1708.

[31] R.S.Falk,G.R. Richter. Local error estimates for a finite element method for hyperbolic and convection-diffusion equations,*SIAM journal on numerical analysis*,**1992**,*29*,730–754.

[32] Richter, G.R.A finite element method for time-dependent convection-diffusion equations,*Mathematics of computation*,**1990**,*54*,81–106.

[33] Y.Tourigny and E. Suli. The finite element method with nodes moving along the characteristics for convection-diffusion equations,*Numer.Math*,**1991**,*59*,399–412.

[34] M.Ono,M.Hane,K. Hane and T.Suzuki. Finite-element analysis of convective diffusion equation for semiconductor problems using conjugate gradient method,*Electronics and Communications in Japan (Part II: Electronics)*,**1988**,*71*,93–99.

[35] T.Zhang and Y. Chen. An analysis of the weak Galerkin finite element method for convection–diffusion equations,*Applied Mathematics and Computation*,**2019**,*346*,612–621.

[36] H.Reinhardt and W. Wendland. A-posteriori error analysis and adaptive finite element methods for singularly perturbed convection-diffusion equations,*Mathematical Methods in the Applied Sciences*,**1982**,*4*,529–548,

[37] E.D.Karepova,V.V.Shaidurov. Fitted scheme of the finite element method for a convection-diffusion equation,*Russian Journal of Numerical Analysis and Mathematical Modelling*,**2000**,*15*,167–182.

[38] R.J.Schnipke and J.G. Rice. A finite element method for free and forced convection heat transfer,*International journal for numerical methods in engineering*,**1987**,*24*,117–128.

[39] P.Nithiarasu,K.N.Seetharamu and T.Sundararajan.Finite element modelling of flow, heat and mass transfer in fluid saturated porous media, *Archives of Computational Methods in Engineering*,**2002**,*9*,3.

[40] T.Zhang and L. Zheng. A finite volume method for Stokes problems on quadrilateral meshes,*Comput. Math. Appl.*, **2019**, *77*, 1091–1106.

[41] H.K.Versteeg and W.Malalasekera. *An introduction to computational fluid dynamics: the finite volume method*;Pearson education: 2007.

[42] D.Pan and C.H. Chang. Upwind finite-volume method for natural and forced convection, *Numerical Heat Transfer, Part B Fundamentals* ,**1994** ,*25*,177–191.

[43] K.Morton,M. Stynes and E. Suli. Analysis of a cell-vertex finite volume method for convection-diffusion problems,*Mathematics of computation*,**1997** ,*66* ,1389–1406.

[44] D.Causona,C. Mingham and L.Qia. *Introductory Finite Volume Methods for PDEs*; Manchester Metropolitan University:UK, **2011**.

[45] A.Hussain,Z.S. Zheng and E.F. Anley. Numerical Analysis of Convection–Diffusion Using a Modified Upwind Approach in the Finite Volume Method ,*Mathematics*,**2020**,*8*,1869.

[46] E.M.Lemos, A.R.Secchi and E.C. Biscaia Jr. Development of high-order finite volume method with multiblock partition technique,*Brazilian Journal of Chemical Engineering*,**2012**,*29*,183–201.

[47] J.H.M.ten TB and M.J.H Anthonissen. The finite volume-complete flux scheme for advection-diffusion-reaction equations,*J. Sci. Comput.*,**2011**,*46*,47–70.

[48] M.Xu. A modified finite volume method for convection-diffusion-reaction Problems,*Int. J. Heat Mass Transfer*,**2018**,*117*,658–668.

[49] R.B.Kinney and H.S.Mahdi. A new finite-volume approach with adaptive upwind convection, *Int. J. Numer. Meth. Engrg.*,**1988** ,*26* ,1325–1343.

[50] H.Wang and W.Zhao. An upwind finite volume scheme and its maximum-principle-preserving ADI splitting for unsteady-state advection-diffusion equations,*Num. Methods Partial Differ. Equ.: An International Journal*,**2003** ,*19* ,211–226.

[51] L.A.Krukier,O.A.Pichugina and B.L.Krukier. Numerical solution of the steady convection-diffusion equation with dominant convection,*Procedia Computer Science*,**2013**,*18*,2095–2100.

[52] G.Birkhoff,E.C. Gartland,Jr and R.E Lynch.Difference methods for solving convection-diffusion equations,*Computers & Mathematics with Applications*,**1990**,*19*,147–160.

[53] J.Douglas,Jr and T.F. Russell. Numerical methods for convection-dominated diffusion problems based on combining the method of characteristics with finite element or finite difference procedures, *SIAM Journal on Numerical Analysis*,**1982**,*19*,871–885.

[54] S.Wang. Solving convection-dominated anisotropic diffusion equations by an exponentially fitted finite volume method,*Computers & Mathematics with Applications*,**2002**,*44*,1249–1265.

[55] Z.W.Cao,Z.F. Liu, Liu and X.H.Wang. A Self-Adaptive Numerical Method to Solve Convection-Dominated Diffusion Problems,*Mathematical Problems in Engineering*, **2017**, *2017*,13

[56] E.F. Anley. Numerical solutions of elliptic partial differential equations by using finite volume method, *Pure and Applied Mathematics Journal*, **2015**, *5*(4), 120–129.

[57] J.C.Heinrich and Ch.C.Yu.On the solution of the time-dependent convection-diffusion equation by the finite element method, *Advances in Water Resources*,**1987** , *10* , 220–224.